Solomon, I., & Bloembergen, N. (1956) *J. Chem. Phys. 25*, 261.
Stewart, J. M. M., & Grisham, C. M. (1988) *Biochemistry 27*, 4840–4848.
Stewart, J. M. M., Jørgensen, P. L., & Grisham, C. M. (1989) *Biochemistry 28*, 4695–4701.
Viswamitra, M. A., Hosur, M. V., Shakked, Z., & Kennard, O. (1976) *Cryst. Struct. Commun. 5*, 819.

EPR Characterization of Genetically Modified Reaction Centers of *Rhodobacter capsulatus*†

Edward J. Bylina,‡,§ Stephen V. Kolaczkowski,‖,⊥ James R. Norris,‖ and Douglas C. Youvan*,‡
Department of Chemistry, Massachusetts Institute of Technology, Cambridge, Massachusetts 02139, and Chemistry Division, Argonne National Laboratory, Argonne, Illinois 60439
Received October 3, 1989; Revised Manuscript Received March 9, 1990

ABSTRACT: Electron paramagnetic resonance (EPR) has been used to investigate the cation and triplet states of *Rhodobacter capsulatus* reaction centers (RCs) containing amino acid substitutions affecting the primary donor, monomeric bacteriochlorophylls (Bchls), and the photoactive bacteriopheophytin (Bphe). The broadened line width of the cation radical in $His^{M200} \rightarrow Leu$ and $His^{M200} \rightarrow Phe$ reaction centers, whose primary donor consists of a Bchl–Bphe heterodimer, indicates a highly asymmetric distribution of the unpaired electron over the heterodimer. A T_0 polarized triplet state with reduced yield is observed in heterodimer-containing RCs. The zero field splitting parameters indicate that this triplet essentially resides on the Bchl half of the heterodimer. The cation and triplet states of reaction centers containing $His^{M200} \rightarrow Gln$, $His^{L173} \rightarrow Gln$, $Glu^{L104} \rightarrow Gln$, or $Glu^{L104} \rightarrow Leu$ substitutions are similar to those observed in wild type. Oligonucleotide-mediated mutagenesis has been used to change the histidine residues that are positioned near the central Mg^{2+} ions of the reaction center monomeric bacteriochlorophylls. Reaction centers containing serine substitutions at M180 and L153 or a threonine substitution at L153 have unaltered pigment compositions and are photochemically active. The cation and triplet states of $His^{L153} \rightarrow Leu$ reaction centers are similar to those observed in wild type. Triplet energy transfer to carotenoid is not observed at 100 K in $His^{M180} \rightarrow Arg$ chromatophores. These results have important implications for the structural requirements of tetrapyrrole binding and for our understanding of the mechanisms of primary electron transfer in the reaction center.

The photosynthetic reaction center (RC) mediates extremely efficient electron-transfer reactions that result in high quantum yields for the conversion of light to chemical energy (Kirmaier & Holten, 1987; Okamura et al., 1982). Crystal structures have been determined for RCs from both *Rhodopseudomonas viridis* (Deisenhofer et al., 1984, 1985) and *Rhodobacter sphaeroides* (Chang et al., 1986; Allen et al., 1986). Although the crystal structure of RCs from *Rhodobacter capsulatus* has not been determined, extensive sequence similarities among these three species [see review in Komiya et al. (1988)] facilitate mutagenesis experiments in *Rb. capsulatus*. Genetic tools are most advanced for this species (Scolnik & Marrs, 1987). RC and light-harvesting genes have been deleted from the *Rb. capsulatus* chromosome (Youvan et al., 1985). Such deletions may be complemented by plasmids (Bylina et al., 1986, 1989) bearing either wild-type or mutagenized copies of the RC genes. Recently, mutations affecting the properties of the primary donor in RCs of *Rb. capsulatus* have been generated and characterized. The primary donor in $His^{M200} \rightarrow Leu$ and $His^{M200} \rightarrow Phe$ reaction centers consists of a heterodimer of bacteriochlorophyll (Bchl) and bacteriopheophytin (Bphe) (Bylina & Youvan, 1988). Time-resolved optical measurements indicate that the quantum yield of the initial electron-transfer reaction in $His^{M200} \rightarrow Leu$ reaction centers is reduced by about half (Kirmaier et al., 1988). Substitutions at glutamic acid residue L104, which interacts with the photoactive Bphe, indicate that glutamic acid-L104 is largely responsible for the spectroscopic red shift of this pigment but that the interaction is not the dominant contributor to the directionality of electron transfer in reaction centers (Bylina et al., 1988b).

Histidines-L153 and -M180 of the *Rps. viridis* reaction center act as axial ligands to the central Mg^{2+} ions of the monomeric Bchl molecules, which are in van der Waals contact with both the primary donor (special pair Bchls) and the RC Bphes (Michel et al., 1986). Refined crystallographic data (Yeates et al., 1988) from *Rb. sphaeroides* suggest that while the M-subunit histidines act as axial ligands to their associated Bchls, the L-subunit histidines (L153 and L173) associated with RC Bchls do not directly ligand the Bchl Mg. One of these monomeric Bchls can be removed from *Rb. sphaeroides* reaction centers by treatment with $NaBH_4$, resulting in the reduction of the ground-state absorption band at 800 nm while leaving the remainder of the absorption spectrum unaffected (Ditson et al., 1984). Reaction center photochemistry is

† This work was supported by the National Science Foundation (DMB-8609614) and the U.S. Department of Agriculture (87-CRCR-1-2328). Work at ANL was supported by the U.S. Department of Energy, Office of Basic Energy Sciences, Division of Chemical Sciences, under Contract W-31-109-Eng-38.
* Address correspondence to this author.
‡ Massachusetts Institute of Technology.
§ Present address: Biotechnology Program, Pacific Biomedical Research Center, University of Hawaii at Manoa, Honolulu, HI 96822.
‖ Argonne National Laboratory.
⊥ Present address: Department of Chemistry, University of Arizona, Tucson, AZ 85721.

0006-2960/90/0429-6203$02.50/0

unaffected in these chemically modified complexes, suggesting that one of the Bchls is neither strongly coupled to the other chromophores nor necessary for electron transfer (Maroti et al., 1985). The removal of monomeric $Bchl_M$ is accompanied by cleavage of the M subunit (Beese et al., 1988). The actual role of these accessory Bchls in electron transfer has not yet been determined. The recent observation of a resolved intermediate state in which electron transfer to the monomeric $Bchl_L$ precedes Bphe reduction at room temperature (Holzapfel et al., 1989) conflicts with earlier experiments in which no such intermediate was observed (Kirmaier & Holten, 1987; Breton et al., 1988).

While the crystal structure can provide spatial information about reaction center chromophores, magnetic resonance spectroscopy yields detailed information on the electronic structure of these pigments, which is important for understanding reaction center function. EPR experiments led to the proposal of the dimeric nature of the primary donor (Norris et al., 1971), helped identify the primary acceptor as a ubiquinone–iron complex (Feher & Okamura, 1976), and suggested that a radical pair intermediate state is present between the electron-transfer step from primary donor to primary acceptor (Thurnauer et al., 1975). More recently, magnetic resonance studies have been extended to single crystals of reaction centers (Norris et al., 1987, 1989). In this paper, electron paramagnetic resonance (EPR) has been used to investigate the cation and triplet states of genetically modified reaction centers of *Rhodobacter capsulatus*.

Materials and Methods

DNA Methods. All procedures were essentially as described by Maniatis et al. (1982). M13 phage were maintained in *Escherichia coli* strain JM103. Plasmid pU29 derivatives were maintained in *E. coli* strain HB101. Plasmid pU2922 derivatives were conjugated from *E. coli* S17-1 donors (Simon et al., 1983).

Mutagenesis. Mutations were generated with a modification (Bylina & Youvan, 1987) of the two-primer method of Zoller and Smith (1984). YIB11, an M13mp18 derivative containing the 1375 base pair *Eco*RI–*Kpn*I fragment of pU29 (Bylina et al., 1986), was used for constructing $His^{L153} \rightarrow Arg$. The $His^{L153} \rightarrow Arg$ mutation introduces a *Mlu*I site at the L153 codon. The template containing the $His^{L153} \rightarrow Arg$ mutation was used for construction of $His^{L153} \rightarrow Leu$, $His^{L153} \rightarrow Ser$, and $His^{L153} \rightarrow Thr$. YIB9, an M13mp18 derivative containing the 929 base pair *Kpn*I–*Bam*HI fragment of pU29 (Bylina et al., 1986), was used for construction of $His^{M180} \rightarrow Ser$. The $His^{M180} \rightarrow Ser$ mutation introduces an *Xho*I site at the M180 codon. The template containing the $His^{M180} \rightarrow Ser$ mutation was used for construction of $His^{M180} \rightarrow Arg$ and $His^{M180} \rightarrow Leu$. DNA inserts were shuttled into pU29 derivatives as described (Bylina & Youvan, 1987). The shuttling of $His^{M180} \rightarrow Ser$ into pU29 was verified by the presence of an additional *Xho*I site. The shuttling of $His^{M180} \rightarrow Arg$ and $His^{M180} \rightarrow Leu$ into pU29($His^{M180} \rightarrow Ser$) was verified by the loss of this *Xho*I site. The shuttling of $His^{L153} \rightarrow Arg$ was verified by the presence of the *Mlu*I site. The shuttling of $His^{L153} \rightarrow Leu$, $His^{L153} \rightarrow Ser$, and $His^{L153} \rightarrow Thr$ into a pU29 derivative (which contains a *Bam*HI site at the L228 codon) was verified by the loss of the *Bam*HI site. The double serine mutation ($His^{L153,M180} \rightarrow Ser$) was constructed by shuttling $His^{M180} \rightarrow Ser$ into pU29($His^{L153} \rightarrow Ser$) and was verified by the presence of an additional *Xho*I site. RC mutations were introduced into pU2922 as described (Bylina et al., 1989). Antisense oligonucleotides were synthesized by using an Applied Biosystems 381A synthesizer.

Phenotypic Assays. RC mutations carried on pU2922 derivatives were conjugated into *Rb. capsulatus* as described (Bylina et al., 1989). *Rb. capsulatus* deletion strain U43 (which lacks the RC and both light-harvesting complexes) served as the background (Youvan et al., 1985) for the determination of mutant phenotypes. *Rb. capsulatus* cultures were grown semiaerobically in supplemented RCV medium (Yen & Marrs, 1977). Photosynthetic growth assays were performed as described (Bylina & Youvan, 1988). Mutants which grew within 2 days under a light intensity of approximately 20 mW/cm^2 were considered photosynthetically competent.

RC Preparation and Analysis. RCs were purified with a modified (Bylina & Youvan, 1988) DEAE chromatography procedure (Prince & Youvan, 1987). Optical spectra were recorded with a Perkin-Elmer λ diode array Model 3840 spectrophotometer linked to a Perkin-Elmer Model 7300 workstation. RC pigment ratios were determined (Straley et al., 1973; van der Rest & Gingras, 1974) by analyzing the near-infrared pigment bands after the extraction of RCs with acetone/methanol, 7:2 (v/v). The extinction coefficients necessary for determination of the pigment ratios have been previously reported for Bchl and Bphe in organic solvents (van der Rest & Gingras, 1974).

EPR Analysis. Electron spin resonance spectra were recorded on a Varian E102 spectrometer, equipped with an Air Products flow-through helium cryostat. EPR measurements were made on chromatophores resuspended in 20 mM Tris-HCl (pH 8). The line widths of the oxidized primary donor were obtained from light-minus-dark difference spectra. Chromatophores were examined at 80 K with 0.5 mW of applied power and a modulation of 0.1 G.

For the EPR spectra of the triplet state of the primary donor in both chromatophores and purified RCs, the primary quinones of the RCs were reduced with a slight excess of sodium dithionite in the EPR sample tubes in a N_2 drybox. The concentration of wild-type RCs was typically 30 μM, while the $His^{M200} \rightarrow Leu$ and $His^{M200} \rightarrow Phe$ RCs were nearly 300 μM. The chromatophore samples had an absorbance of 50 (1 cm path), as measured at 875 nm. The triplet EPR spectra were obtained with 5-mW incident microwave power, 9.16 GHz, 1000-G scan width, modulation amplitude 8 G at 6 K. The spectra were repeatedly scanned to improve the signal to noise. The RCs were illuminated through the dewar of the He(l)-cooled cryostat in the microwave cavity with the filtered output (500–1000 nm) from an electronically modulated, 500-Hz, Xe arc lamp. The output from the spectrometer was amplified with an EG&G 5208 lock-in amplifier using a signal from the sync output of the lamp power modulator as the lock-in frequency. The phase angle of the lock-in amplifier was initially set by using *Rb. sphaeroides* R-26 RCs as the control sample. The phase angle was then maximized for each of the modified *Rb. capsulatus* RCs (in chromatophores or purified RCs). In every case, the maximum signal to noise ratio for the modified *Rb. capsulatus* RCs was obtained with a phase angle setting within 5° of the value obtained for the *Rb. sphaeroides* R-26 sample. The relative decay rates of the three triplet sublevels can be determined from the phase angle dependence of the lock-in amplifier for each set of X, Y, and Z peaks (Paul, 1976; Thurnauer, 1979; Levanon & Norris, 1978).

Results

Mutations Affecting the Monomeric Bchls. The histidine residues associated with the central Mg of the monomeric Bchls were changed by site-directed mutagenesis (Table I).

Table I: Directed Mutations of the Axial Histidine Ligands of Monomeric Bchls of the RC[a]

mutation	nucleotide change	Bchl/ Bphe ratio	photosynthetic growth
wild type		1.9 ± 0.1	+
$His^{L153} \rightarrow Arg$	CAC → CGT	nd	−
$His^{L153} \rightarrow Leu$	CAC → CTC	nd	+
$His^{L153} \rightarrow Ser$	CAC → TCC	2.0 ± 0.1	+
$His^{L153} \rightarrow Thr$	CAC → ACC	2.0 ± 0.1	+
$His^{M180} \rightarrow Arg$	CAC → CGC	nd	−
$His^{M180} \rightarrow Leu$	CAC → CTC	nd	+
$His^{M180} \rightarrow Ser$	CAC → AGC	1.9 ± 0.1	+
$His^{L153,M180} \rightarrow Ser$		2.1 ± 0.1	+

[a] Nomenclature such as $His^{M180} \rightarrow Ser$ includes the wild-type residue (histidine), the subunit and position of this residue (amino acid 180 of the M subunit), and the newly incorporated residue (serine). The nucleotide sequences given in the table are of the mutagenized codon. Pigment extraction data reported are the average of a minimum of three trials. See Materials and Methods for photosynthetic growth conditions. nd = not determined.

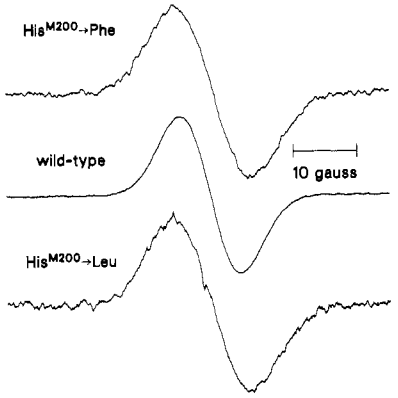

FIGURE 1: EPR signals of the photooxidized primary donor in wild-type, $His^{M200} \rightarrow Leu$, and $His^{M200} \rightarrow Phe$ chromatophores. The primary donors were examined at 80 K with 0.5-mW applied power and a modulation amplitude of 0.1 G. These are light-minus-dark difference spectra.

His^{L153} was changed to arginine, leucine, serine, and threonine, whereas His^{M180} was changed to arginine, leucine, and serine. A double mutant was constructed in which both histidines were replaced with serine ($His^{L153,M180} \rightarrow Ser$). Absorption spectra of chromatophore membranes from each of these mutants show that in each case the reaction center is present in the membrane (data not shown). In the light-harvesting II-deficient background U43, reaction center absorption at 750 and 800 nm (along with light-harvesting I absorption at 875 nm) is seen in chromatophores from each of the mutants. The $His^{L153} \rightarrow Leu$, $His^{L153} \rightarrow Ser$, $His^{L153} \rightarrow Thr$, $His^{M180} \rightarrow Leu$, $His^{M180} \rightarrow Ser$, and $His^{L153,M180} \rightarrow Ser$ mutants are all photosynthetically competent, which indicates that they contain functional reaction centers.

Line Width of the Oxidized Primary Donor. The EPR spectrum of the oxidized primary donor in chromatophores containing wild-type RCs from *Rhodobacter capsulatus* is shown in Figure 1. The line width of this light-minus-dark difference signal is 9.5 G. The line width of purified reaction centers (Figure 2) is 10.6 G, similar to the value reported previously (Prince & Youvan, 1987). No $g = 2$ signal is observed in the dark for these purified wild-type reaction centers (data not shown). The observed broadening may be related to the 20-nm blue shift of the wild-type *Rb. capsulatus* special pair absorption band following purification (Prince & Youvan, 1987).

The primary donor in RCs where leucine or phenylalanine replaces the special pair Bchl binding histidine at M200

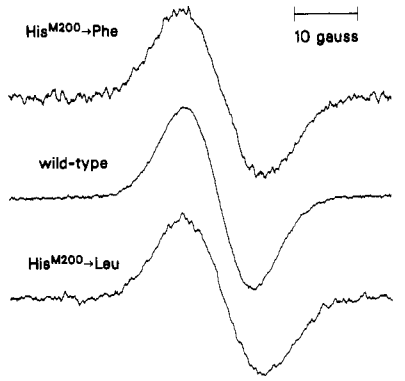

FIGURE 2: EPR signals of the photooxidized primary donor in purified wild-type, $His^{M200} \rightarrow Leu$, and $His^{M200} \rightarrow Phe$ RCs. The primary donors were examined at 5 K with 0.5-mW applied power and a modulation amplitude of 0.1 G. These are light-minus-dark difference spectra.

Table II: EPR Line Widths of the Oxidized Primary Donor and Zero Field Splitting Parameters of the Primary Donor Triplet State for Genetically Modified RCs[a]

mutation	line width of oxidized primary donor (G)	ZFS parameters (cm^{-1}) $\lvert D\rvert$	$\lvert E\rvert$
chromatophores			
wild type	9.5	0.0189	0.0032
$His^{M200} \rightarrow Leu$	12.2	nd	nd
$His^{M200} \rightarrow Phe$	12.0	nd	nd
$His^{M200} \rightarrow Gln$	9.3	0.0190	0.0034
$His^{L173} \rightarrow Gln$	9.8	0.0188	0.0033
$His^{L173,M200} \rightarrow Gln$	9.5	0.0190	0.0036
$Glu^{L104} \rightarrow Gln$	9.5	0.0188	0.0032
$Glu^{L104} \rightarrow Leu$	9.5	0.0188	0.0032
$His^{L153} \rightarrow Leu$	9.7	0.0189	0.0033
$His^{L153} \rightarrow Ser$	9.8	0.0189	0.0033
$His^{L153} \rightarrow Thr$	9.5	0.0189	0.0032
$His^{M180} \rightarrow Arg$	9.9	0.0191	0.0033
$His^{M180} \rightarrow Leu$	9.5	0.0190	0.0032
$His^{M180} \rightarrow Ser$	9.5	0.0190	0.0032
purified reaction centers			
wild type	10.6	0.0196	0.0035
$His^{M200} \rightarrow Leu$	12.6	0.0210	0.0060
$His^{M200} \rightarrow Phe$	12.3	0.0213	0.0061

[a] The ZFS $\lvert D\rvert$ value was determined from the Z turning point ↔ Z turning point separation. The ZFS $\lvert E\rvert$ value is the average of $\lvert E\rvert$ values determined from the X turning point ↔ X turning point and the Y turning point ↔ Y turning point separations, with the exception of heterodimer-containing RCs, where only the Y turning point ↔ Y turning point separation was used. Uncertainty in the line widths is ±0.3 G. Uncertainty in $\lvert D\rvert$ and $\lvert E\rvert$ is ±0.0001 cm^{-1}, except for heterodimer-containing RCs, where the uncertainty is ±0.0010 cm^{-1}. nd = not determined.

consists of a Bchl–Bphe heterodimer. A broad diffuse band replaces the wild-type special pair absorption band at 850 nm in the optical absorption spectrum of $His^{M200} \rightarrow Leu$ RCs (Bylina & Youvan, 1988). The light-minus-dark EPR difference spectra of the oxidized primary donor in $His^{M200} \rightarrow Leu$ and $His^{M200} \rightarrow Phe$ chromatophores are shown in Figure 1. The signals are centered at the same g value observed for wild type, but are much broader (12.2 and 12.0 G, respectively). The EPR difference spectra for the purified RCs are shown in Figure 2. The line widths are slightly broader than those observed in chromatophores (Table II), similar to the case for wild type. No $g = 2$ signal is observed in the dark for the purified RCs of $His^{M200} \rightarrow Leu$ (data not shown).

The EPR line widths of the oxidized primary donors in chromatophore preparations that contain RCs with other genetically modified protein–tetrapyrrole interactions are listed in Table II. These RCs contain amino acid substitutions

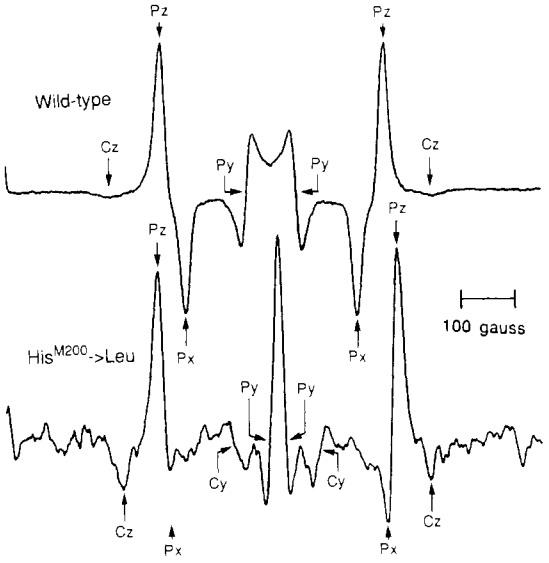

FIGURE 3: Triplet EPR spectra of wild-type and heterodimer-containing His^{M200} → Leu RCs at 6 K. The primary donor triplet spectral turning points are labeled P_z, P_x, and P_y, and the carotenoid Z turning points are labeled C_z. Note that the C_z signals are quite prominent in the heterodimer RC spectrum as compared to the wild-type spectrum.

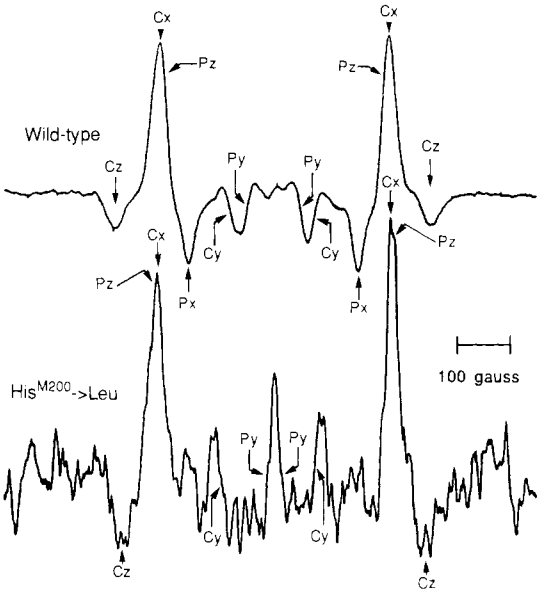

FIGURE 4: Triplet EPR spectra of wild-type and heterodimer-containing His^{M200} → Leu RCs at 100 K. The primary donor triplet signals are labeled P_z, P_x, and P_y, and the carotenoid signals are identified C_z, C_x, and C_y (Chadwick & Frank, 1986). Note that the splitting between the C_x turning points in this spectrum is less than the $P_z \leftrightarrow P_z$ splitting of the same RCs in Figure 3. The absence of the heterodimer P_x turning points is due to the large width of the C_x signals at the same field position.

affecting the environment of the special pair, the monomeric Bchls, and the photoactive Bphe. With the exception of the heterodimer-containing RCs, alterations in the protein environment of the RC tetrapyrrole molecules have relatively little effect on the primary donor radical cation state. For each of these mutations, (1) the observed line width of the oxidized primary donor is similar to that found in chromatophores containing wild-type RCs, and (2) the signals are centered at the same g value observed for wild type.

Photoexcited Triplet State. The EPR spectrum of the primary donor triplet state of wild-type *Rb. capsulatus* RCs is shown in Figure 3. The zero field splitting (ZFS) parameters $|D|$ and $|E|$ are 0.0196 and 0.0035 cm^{-1}, respectively. The values of these parameters in chromatophores containing wild-type reaction centers are 0.0189 and 0.0032 cm^{-1}. Similar small differences have been previously observed in *Rb. capsulatus* (Prince & Youvan, 1987).

The EPR spectrum of the triplet-state heterodimer primary donor (Figure 3) is significantly altered relative to the EPR spectrum obtained for the wild-type triplet primary donor. The polarization pattern of a triplet state describes whether the individual EPR signals (listed in order from low field to high field) are absorbing or emitting microwaves. The T_0, radical pair, polarization pattern for the six turning points in the wild-type reaction center spectrum is (a,e,e,a,a,e), whereas the corresponding pattern for the heterodimer primary donor is (a,?,e,a,a,e). Because of the weak signals observed for the heterodimer RCs, the second turning point is not observed. As a result of the overall agreement between the polarization patterns, we conclude that the heterodimer triplet state is T_0 polarized and arises from the back-reaction of the initial radical pair [i.e., $(Bchl)_2^+Bphe^- \rightarrow {}^3*(Bchl)_2Bphe$ in wild-type RCs and $(Bchl\text{-}Bphe)^+Bphe^- \rightarrow {}^3*(Bchl\text{-}Bphe)Bphe$ in heterodimer-containing RCs]. These polarization patterns for the homodimer and heterodimer are independent of the phase angle settings on the lock-in amplifier. Changes in the phase angle of less than 90° reduce the intensity of the P_z peaks of the heterodimer primary donor triplet in a manner that indicates that P_z decays more slowly than P_x and P_y. Both the phase angle dependence and the light modulation frequency dependence of the heterodimer triplet signals indicate that the individual heterodimer triplet-state spin sublevels decay to the ground state with approximately the same rate constants as the wild-type RCs.

The intensities of the triplet signals in the heterodimer-containing RCs are greatly reduced relative to those observed in wild-type RCs. We were unable to obtain spectra of the primary donor triplet state with acceptable signal-to-noise ratios using chromatophores containing His^{M200} → Leu or His^{M200} → Phe RCs. The reaction center concentration, receiver gain, and the number of signals averaged to obtain the spectrum for His^{M200} → Leu RCs in Figure 3 were all significantly larger than those used to obtain the *Rb. capsulatus* wild-type spectrum. Signals from the triplet carotenoid are observed to contribute to the His^{M200} → Leu triplet spectrum at 6 K. This leads to consideration of the overlap of the carotenoid X turning point, C_x, with the heterodimer P_z turning point. Triplet energy transfer from the primary donor to the carotenoid is a temperature-dependent process. The triplet-state EPR spectra of RCs from wild-type and His^{M200} → Leu measured at 100 K (where the carotenoid triplet signal is enhanced) are shown in Figure 4. These spectra show (Chadwick & Frank, 1986) that the $X \leftrightarrow X$ splittings of the carotenoid triplet signals in wild-type and His^{M200} → Leu RCs are identical. These data also show that although the C_x turning points do overlap with the P_z turning points of both the wild-type and His^{M200} → Leu primary donor triplet states, it is possible to separate the contribution of the carotenoid signal from the primary donor signals. Therefore, the ZFS $|D|$ values of the primary donor triplet states in the His^{M200} → Leu and His^{M200} → Phe RCs can be assigned unambiguously as 0.0210 ± 0.0010 cm^{-1} (see Table II). The zero field splitting $|E|$ values for the two heterodimer-containing RCs, 0.0060 ± 0.0010 cm^{-1}, are obtained from the width of the central peak in the heterodimer-containing RC spectra. In principle, the ZFS $|E|$ value can also be obtained from the X ↔ X splittings of the primary donor triplet signals. However, the relatively large $|E|$ value causes the X turning points to overlap the Z turning points in the primary donor triplet

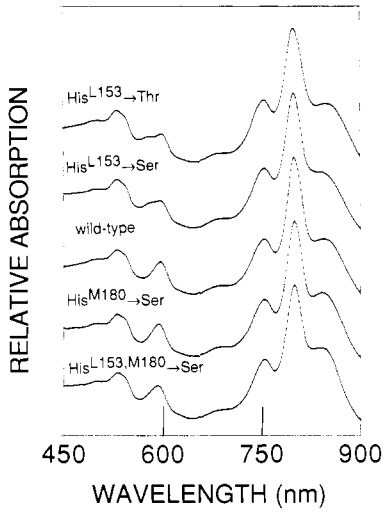

FIGURE 5: Room temperature ground-state absorption spectra of genetically altered RCs affecting the monomeric bridging Bchls.

spectra of heterodimer RCs. For the His^{M200} → Leu RC spectrum shown in Figure 3, only the high-field X turning point is readily observed.

The ZFS parameters of the triplet state in chromatophores containing reaction centers with other genetically modified protein–tetrapyrrole interactions are listed in Table II. In each case, the primary donor triplet state is readily observed in the chromatophore preparations, and the observed ZFS $|D|$ and $|E|$ values are similar to values determined for chromatophores containing wild-type RCs. In chromatophores from His^{M180} → Arg, triplet energy transfer from the primary donor to the carotenoid is not observed in the 6–100 K temperature range (data not shown).

Characterization of Reaction Centers Containing Mutations at L153 and M180. RCs were purified from the chromatophore membranes of His^{L153} → Ser, His^{L153} → Thr, His^{M180} → Ser, and His^{L153,M180} → Ser. We were unable to purify photochemically active RCs from His^{L153} → Arg and His^{L153} → Leu. Photochemically active RCs were purified from His^{M180} → Arg and His^{M180} → Leu; however, the RCs were isolated in low yields and with variable absorption spectra (data not shown). A large reduction in the RC 850-nm absorption band is observed when His^{L153} → Thr chromatophores are solubilized in 1.5% LDAO. RCs with wild-type 850-nm levels can be obtained by reducing the LDAO concentration used for solubilization, but the species giving rise to the 850-nm absorption band is unstable, varying between preparations and disappearing after brief storage of the samples on ice. A similar instability in the 850-nm absorption band was observed in RCs containing the His^{L173} → Gln mutation (Bylina & Youvan, 1988). RCs containing serine substitutions at either L153 and M180 remain stable during purification.

The room temperature absorption spectra of RCs isolated from His^{L153} → Ser, His^{L153} → Thr, His^{M180} → Ser, and His^{L153,M180} → Ser are shown in Figure 5. The lowest energy singlet electronic transitions of the RC chromophores (Q_y region) near 750, 800, and 850 nm are assigned predominantly to the Bphe Q_y transitions, the monomeric Bchl Q_y transitions, and the special pair Bchl Q_y transitions, respectively. The spectra from these RCs resemble the absorption spectrum from wild-type RCs. Differences between RCs containing mutations at His^{L153} and wild-type RCs can be observed in the Bchl Q_x transitions near 600 nm. Spectral changes and band splitting of this transition are observed in other RCs where Bchl axial histidine ligands have been mutagenized (Bylina & Youvan, 1988, and unpublished observations).

Pigment extractions were performed on RCs from His^{L153} → Ser, His^{L153} → Thr, His^{M180} → Ser, and His^{L153,M180} → Ser and wild type to determine their pigment content. The Bchl/Bphe ratios for these reaction centers are listed in Table I. The ratios for both wild-type and mutagenized reaction centers are in good agreement with the expected Bchl/Bphe ratio of 2. Considering these pigment ratios and the similarities of the absorption spectra with wild type, we conclude that these mutations do not alter the pigment composition of *Rb. capsulatus* RCs.

Discussion

Properties of the Heterodimer. We have shown that the magnetic properties of the primary donor in Bchl–Bphe heterodimer-containing RCs are different than the properties of Bchl–Bchl homodimer wild-type RCs. No dark EPR signal is observed in heterodimer-containing RCs, suggesting that these purified RCs are not partially oxidized and that the ground state of the heterodimer is not a charge-separated state ($Bchl^+Bphe^-$). The 12.6-G line width in His^{M200} → Leu and His^{M200} → Phe RCs indicates that the radical cation state of the primary donor is monomeric in nature. In view of the different redox properties of Bchl and Bphe, this asymmetry is expected (Bylina & Youvan, 1988). Since Bchl is easier to oxidize than Bphe (Fajer et al., 1975), the positive charge of the primary donor cation probably resides on the Bchl component of the heterodimer.

The ZFS parameters of the heterodimer triplet are similar to those observed for Bchl *a* in vitro (Thurnauer, 1979), suggesting that the triplet, like the radical cation, resides on the Bchl half of the heterodimer. This indicates that the chemical differences between the Bchl and Bphe halves of the heterodimer have an important influence in the quantum description of the heterodimer. The large ZFS $|E|$ value for the heterodimer-containing RCs explains the partial obscuring of the X turning points in the heterodimer triplet spectrum.

A second important difference observed about the triplet state of the heterodimer is the apparent large reduction in triplet yield. We interpret the weak signals observed for the heterodimer triplet state as indicating an overall reduction in the triplet yield. The small signals (with relatively poor signal-to-noise ratio) observed for the heterodimer-containing RCs at several light modulation frequencies at 6 K indicate that, on average, significantly fewer ^{3}(Bchl–Bphe) states are present in the sample than are observed for RCs from either wild-type *Rb. capsulatus*, wild-type *Rb. sphaeroides*, or *Rb. sphaeroides* strain R-26. Since the heterodimer triplet is T_0-polarized, the radical pair mechanism that is used to describe the formation of the triplet state in wild-type RCs is also applicable to triplet formation in the heterodimer-containing RCs. The radical pair mechanism has been extensively reviewed, and the triplet yield can be approximated by eq 1

$$\Phi_T = k_t\omega/[\omega(k_s + k_t) + k_sk_t] \quad (1)$$

where k_s represents the rate of radical pair recombination from the singlet state, k_t represents the rate of radical pair recombination from the triplet state, and ω is a classical rate constant approximating the rate of singlet–triplet interconversion in the radical pair (Budil, 1986; Budil et al., 1987; Ogrodnik et al., 1987). Equation 1 shows that the triplet yield of the radical pair mechanism will decrease with increases in k_s or decreases in k_t and ω. In an effort to identify the most probable cause for the reduced triplet yield in heterodimer-containing RCs, experiments to determine k_s, k_t, and ω (Budil et al., 1987; Kolaczkowski et al., 1987) have been initiated. We have

observed an overall decrease in the total combined radical pair lifetime, both ^{1}[(Bchl–Bphe)$^+$Bphe$^-$] and ^{3}[(Bchl–Bphe)$^+$-Bphe$^-$], as compared to wild-type RCs (Kolaczkowski et al., 1990). This observation suggests that the singlet recombinational rate, k_s, is much larger for the heterodimer-containing RCs than the wild-type RCs. Further experiments, in progress, should resolve this issue.

Specificity of Tetrapyrrole Binding. Histidine residues serve as the axial ligands (Michel et al., 1986) to the central Mg of each of the RC Bchls in *Rps. viridis*. These histidines are conserved (Komiya et al., 1988) in all bacterial RCs characterized to date, with the exception of the M subunit of *Chloroflexus aurantiacus*, where one of the monomeric Bchls is replaced by Bphe (Blankenship et al., 1983) and the corresponding histidine is replaced (Ovchinnikov et al., 1988) with leucine (M171). Recent mutagenesis results indicate that histidine is not required for Bchl binding. Glutamine can replace the histidine residues (L173 and M200) which interact with the "special pair" Bchls (Bylina & Youvan, 1988). The mutations presented here demonstrate that amino acid residues containing hydroxyl groups can also replace these histidine residues. Side chains containing lone pairs of electrons appear to be necessary for Bchl binding, since leucine and phenylalanine substitutions at M200 in *Rb. capsulatus* (Bylina & Youvan, 1988) and the leucine residue found at M171 in *Chloroflexus* (Ovchinnikov et al., 1988) both result in Bphe incorporation. Preliminary pigment extraction data from His^{M180} → Leu RCs suggest an altered pigment composition in these RCs (data not shown). While refined crystallographic data (Yeates et al., 1988) from *Rb. sphaeroides* suggest that the L-subunit histidines (L153 and L173) associated with RC Bchls do not directly ligand the Bchl Mg, these interactions may play an important role in the RC assembly process and in the differentiation of Bchl and Bphe.

Symmetric Mutations. The structure of the L and M subunits and the various prosthetic groups shows an approximate 2-fold symmetry whose axis is perpendicular to the plane of the membrane (Deisenhofer et al., 1985; Komiya et al., 1988). This symmetry is not exact, as demonstrated by the differences in absorption properties of symmetrically related chromophores, the differences in protein environment of these chromophores, and the involvement of only one of the pathways in electron transfer. A comparison of mutations at symmetry-related conserved amino acid residues in the L and M subunits also reveals this break with symmetry. Specifically, mutations at histidines in the L subunit which are located near the Mg^{2+} of Bchls show greater reaction center instability during purification than the corresponding mutations in the M subunit. This difference in RC stability may be related to the differences in Bchl Mg coordination observed in *Rb. sphaeroides* (Yeates et al., 1988). Alternatively, this instability may be caused by the disruption of potential hydrogen bonding interactions (Yeates et al., 1988) between the histidines at L153 or L173 and other L-subunit residues.

Role of Monomeric Bchl in Electron Transfer. Mutations affecting protein–monomeric Bchl interactions will help to better understand the role of these monomeric Bchls in electron transfer and its unidirectionality. While conflicting results have been reported regarding the observation of a resolved intermediate state in which electron transfer to the monomeric $Bchl_L$ precedes Bphe reduction (Kirmaier & Holten, 1987; Breton et al., 1988; Holzapfel et al., 1989), most theoretical models involve the participation of the monomeric $Bchl_L$ either directly or indirectly in electron transfer (Bixon et al., 1987; Marcus, 1988a; Fischer & Scherer, 1987). One mutation

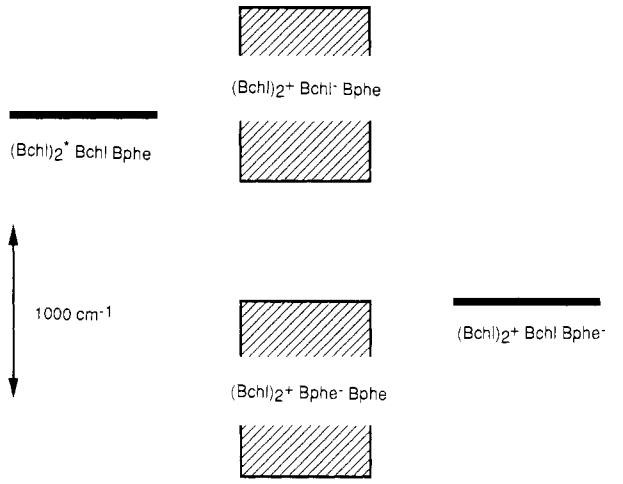

FIGURE 6: Approximate energy diagram for the initial step in electron transfer. The width in the energy levels of $(Bchl)_2^+Bchl_L^-Bphe$ represents the range of values for this state estimated in a variety of theoretical models (Marcus, 1988b; Bixon et al., 1988; Won & Friesner, 1988; Scherer & Fischer, 1987; Creighton et al., 1988). We assume that the $(Bchl)_2{}^*Bphe_LBphe$ and $(Bchl)_2^+Bphe_LBphe^-$ states would be similar in energy to the $(Bchl)_2{}^*Bchl_LBphe$ and $(Bchl)_2^+$-$Bchl_LBphe^-$ states, respectively.

which is expected to affect this energy level of the monomeric $Bchl_L$ anion is His^{L153} → Leu. Replacement of histidine with leucine may result in the substitution of monomeric $Bchl_L$ with Bphe. However, we have been unable to purify RCs containing this mutation, which would allow us to determine its pigment composition and its electron-transfer properties. Since EPR measurements can be made on chromatophores or whole cells, this form of spectroscopy can be used to characterize mutations without isolating RCs. EPR data for His^{L153} → Leu chromatophores indicate that these RCs are photochemically active, since the presence of a $(Bchl)_2^+$ EPR signal indicates that $(Bchl)_2^+Q_A^-$ is stably formed. The line width of the oxidized primary donor and the ZFS parameters of the triplet are similar to those observed in wild type (Table II).

The interpretation of these results is dependent on whether Bchl or Bphe is present at the "monomeric $Bchl_L$ site" in His^{L153} → Leu RCs. If Bchl is bound, the structural parameters which determine tetrapyrrole specificity must be reconsidered. The presence of Bchl is inconsistent with the specificity of tetrapyrrole binding currently observed in RCs (see above). However, if Bchl remains bound as the bridging molecule in His^{L153} → Leu RCs, only slight perturbations in electron transfer would be observed, since changes in the energy state of $(Bchl)_2^+Bchl_L^-Bphe$ caused by this substitution are expected to be small. If Bphe is bound, the role of the monomeric Bchl in electron transfer must be reconsidered. Substitution of Bphe for Bchl as the bridging molecule would have a significant effect on the initial steps in RC electron transfer. Since Bphe is easier to reduce than Bchl by approximately 300 mV (Fajer et al., 1975), a large perturbation in the energy state of $(Bchl)_2^+Bphe_L^-Bphe$ [relative to $(Bchl)_2^+Bchl_L^-Bphe$] is expected. An energy diagram for the initial steps in electron transfer is shown in Figure 6. In both the superexchange and intermediate acceptor models (Marcus, 1988b; Bixon et al., 1988; Won & Friesner, 1988; Scherer & Fischer, 1987; Creighton et al., 1988), the $(Bchl)_2^+Bchl_L^-Bphe$ state in wild type is close in energy to $(Bchl)_2{}^*$ (Figure 6). The lowering of the energy of the $(Bchl)_2^+Bphe_L^-Bphe$ state below that of $(Bchl)_2{}^*$ should result in the resolution of this state as an intermediate in the charge separation event. However, the stabilization of the $(Bchl)_2^+Bphe_L^-Bphe$ state would also result in equivalent energy levels of $(Bchl)_2^+Bphe_L^-Bphe$ and

$(Bchl)_2^+Bphe_L Bphe^-$ [$(Bchl)_2^+Bphe_L^-Bphe$ may even be lower in energy than $(Bchl)_2^+Bphe_L Bphe^-$]. In both models, the equilibrium between charge recombination and Bphe reduction following the formation of $(Bchl)_2^+Bphe_L^-Bphe$ would be expected to favor charge recombination, resulting in a block in electron transfer. In the exciton–charge transfer model, the $(Bchl)_2 Bphe_L^+Bphe^-$ state would be destabilized, also resulting in a block in electron transfer. However, the EPR results indicate that the $His^{L153} \rightarrow$ Leu RCs are photochemically active down to 6 K. The incompatibility of these results with the current theories of the mechanisms of electron transfer in RCs points to the importance of determining the pigment content of $His^{L153} \rightarrow$ Leu RCs.

Photosystem II. The core of the photosystem II reaction center is very similar (Youvan & Marrs, 1984) in structure to the bacterial RCs of the *Rhodospirillaceae*. Photochemically active photosystem II reaction centers have been isolated which includes two polypeptides (D1 and D2) that are homologous to the L and M subunits of bacterial reaction centers (Nambo & Satoh, 1987). Functionally important amino acid residues are conserved between the D1 and D2 proteins of photosystem II and the L and M subunits of photosynthetic bacteria (Michel & Deisenhofer, 1988). One of the major structural differences between these two complexes is that the axial histidine ligands of the monomeric Bchls in bacterial RCs are not conserved in D1 and D2. An examination of the postulated CD interhelical region in D1 shows that a threonine residue is located in the position corresponding to histidine L153. Serine and asparagine residues are also found in this region. Our results suggest that the bacterial model may be valid for the binding of the monomeric Bchl associated with D1 in photosystem II, since serine or threonine can replace the histidine at L153 in the bacterial reaction centers of *Rb. capsulatus*.

Acknowledgments

E.J.B. and D.C.Y. thank Bill Coleman for helpful discussions and a critical reading of the manuscript.

References

Allen, J. P., Feher, G., Yeates, T. O., Rees, D. C., Deisenhofer, J., Michel, H., & Huber, R. (1986) *Proc. Natl. Acad. Sci. U.S.A. 83*, 8589–8593.

Beese, B., Steiner, R., Scheer, H., Angerhofer, A., Robert, B., & Lutz, M. (1988) *Photochem. Photobiol. 47*, 293–304.

Bixon, M., Jortner, J., Michel-Bayerle, M. E., Ogrodnik, A., & Lersch, W. (1987) *Chem. Phys. Lett. 140*, 626–630.

Bixon, M., Michel-Bayerle, M. E., & Jortner, J. (1988) *Isr. J. Chem. 28*, 155–168.

Blankenship, R. E., Feick, R., Bruce, B. D., Kirmaier, C., Holten, D., & Fuller, R. C. (1983) *J. Cell. Biochem. 22*, 251–261.

Breton, J., Martin, J.-L., Fleming, G. R., & Lambry, J. C. (1988) *Biochemistry 27*, 8276–8284.

Breton, J., Bylina, E. J., & Youvan, D. C (1989) *Biochemistry 28*, 6423–6430.

Budil, D. E. (1986) Ph.D. Dissertation, University of Chicago.

Budil, D. E., Kolaczkowski, S. V., & Norris, J. R. (1987) in *Progress in Photosynthetic Research* (Biggins, J., Ed.) Vol. 1, pp 25–28, Martinus Nijoff, Dordrecht, The Netherlands.

Bylina, E. J., & Youvan, D. C. (1987) *Z. Naturforsch., C: Biosci. 42C*, 769–774.

Bylina, E. J., & Youvan, D. C. (1988) *Proc. Natl. Acad. Sci. U.S.A. 85*, 7226–7230.

Bylina, E. J., Ismail, S., & Youvan, D. C. (1986) *Plasmid 16*, 175–181.

Bylina, E. J., Jovine, R., & Youvan, D. C. (1988a) in *The Photosynthetic Bacterial Reaction Center: Structure and Dynamics* (Breton, J., & Vermeglio, A., Eds.) pp 113–118, Plenum Press, New York.

Bylina, E. J., Kirmaier, C., McDowell, L., Holten, D., & Youvan, D. C. (1988b) *Nature 336*, 182–184.

Bylina, E. J., Jovine, R. V. M., & Youvan, D. C. (1989) *Bio/Technology 7*, 69–74.

Chadwick, B. W., & Frank, H. A. (1986) *Biochim. Biophys. Acta 851*, 257–266.

Chang, C.-H., Tiede, D., Tang, J., Smith, U., Norris, J., & Schiffer, M. (1986) *FEBS Lett. 205*, 82–86.

Creighton, S., Hwang, J.-K., Warshel, A., Parson, W. W., & Norris, J. R. (1988) *Biochemistry 27*, 774–781.

Deisenhofer, J., Epp, O., Miki, K., Huber, R., & Michel, H. (1984) *J. Mol. Biol. 180*, 385–398.

Deisenhofer, J., Epp, O., Miki, K., Huber, R., & Michel, H. (1985) *Nature 318*, 618–624.

Ditson, S. L., Davis, R. C., & Pearlstein, R. M. (1984) *Biochim. Biophys. Acta 766*, 623–629.

Evans, T. A., & Katz, J. J. (1975) *Biochim. Biophys. Acta 396*, 414–426.

Fajer, J., Brune, D., Davis, M. S., Forman, A., & Spaulding, L. D. (1975) *Proc. Natl. Acad. Sci. U.S.A. 72*, 4956–4960.

Feher, G., & Okamura, M. Y. (1976) *Brookhaven Symp. Biol. 28*, 183–194.

Fischer, S. F., & Scherer, P. O. J. (1987) *Chem. Phys. 115*, 151–158.

Holzapfel, W., Finkele, U., Kaiser, W., Oesterhelt, D., Scheer, H., Stilz, H. U., & Zinth, W. (1989) *Chem. Phys. Lett. 160*, 1–7.

Kirmaier, C., & Holten, D. (1987) *Photosynth. Res. 13*, 225–260.

Kirmaier, C., Holten, D., Bylina, E. J., & Youvan, D. C. (1988) *Proc. Natl. Acad. Sci. U.S.A. 85*, 7562–7566.

Kolaczkowski, S. V., Budil, D. E., & Norris, J. R. (1987) in *Progress in Photosynthetic Research* (Biggins, J., Ed.) Vol. 1, pp 213–216, Martinus Nijoff, Dordrecht, The Netherlands.

Kolaczkowski, S. V., Bylina, E. J., Youvan, D. C., & Norris, J. R. (1990) in *Molecular Biology of Membrane-Bound Complexes in Phototrophic Bacteria* (Drews, G., Ed.) pp 305–312, Plenum Press, London.

Komiya, H., Yeates, T. O., Rees, D. C., Allen, J. P., & Feher, G. (1988) *Proc. Natl. Acad. Sci. U.S.A. 85*, 9012–9016.

Levanon, H., & Norris, J. R. (1978) *Chem. Rev. 78*, 185–198.

Maniatis, T., Fritsch, E. F., & Sambrook, J. (1982) *Molecular Cloning: A Laboratory Manual*, Cold Spring Harbor Laboratory, Cold Spring Harbor, NY.

Marcus, R. A. (1988a) *Chem. Phys. Lett. 146*, 13–22.

Marcus, R. A. (1988b) *Isr. J. Chem. 28*, 205–214.

Maroti, P., Kirmaier, C., Wraight, C., Holten, D., & Pearlstein, R. M. (1985) *Biochim. Biophys. Acta 810*, 132–139.

Michel, H., & Deisenhofer, J. (1988) *Biochemistry 27*, 1–7.

Michel, H., Epp, O., & Deisenhofer, J. (1986) *EMBO J. 5*, 2445–2451.

Namba, O., & Satoh, K. (1987) *Proc. Natl. Acad. Sci. U.S.A. 84*, 109–112.

Norris, J. R., Uphaus, R. A., Crespi, H. L., & Katz, J. J. (1971) *Proc. Natl. Acad. Sci. U.S.A. 68*, 625–629.

Norris, J. R., Lin, C. P., & Budil, D. E. (1987) *J. Chem. Soc., Faraday Trans. 1 83*, 13–27.

Norris, J. R., Budil, D. E., Gast, P., Chang, C.-H., El-Kabbani, O., & Schiffer, M. (1989) *Proc. Natl. Acad. Sci. U.S.A. 86*, 4335–4339.
Ogrodnik, A., Remy-Richter, N., Michel-Bayerle, M. E., & Feick, R. (1987) *Chem. Phys. Lett. 135*, 576–581.
Okamura, M. Y., Feher, G., & Nelson, N. (1982) in *Photosynthesis: Energy Conversion by Plants and Bacteria* (Govindjee, Ed.) pp 195–272, Academic Press, New York.
Ovchinnikov, Yu. A., Abdulaev, N. G., Schmuckler, B. E., Zargarov, A. A., Kutuzov, M. A., Telezhinskaya, I. N., Levina, N. B., & Zolotarev, A. S. (1988) *FEBS Lett. 232*, 364–368.
Paul, H. (1976) *Chem. Phys. 15*, 115–129.
Prince, R. C., & Youvan, D. C. (1987) *Biochim. Biophys. Acta 890*, 286–291.
Scherer, P. O. J., & Fischer, S. F. (1987) *Chem. Phys. Lett. 141*, 179–185.
Scolnik, P. A., & Marrs, B. L. (1987) *Annu. Rev. Microbiol. 41*, 703–726.
Simon, R., Priefer, U., & Puhler, A. (1983) *Bio/Technology 1*, 784–791.
Straley, S. C., Parson, W. W., Mauzerall, D. C., & Clayton, R. C. (1973) *Biochim. Biophys. Acta 305*, 597–609.
Thurnauer, M. (1979) *Rev. Chem. Intermed. 3*, 197–230.
Thurnauer, M. C., Katz, J. J., & Norris, J. R. (1975) *Proc. Natl. Acad. Sci. U.S.A. 72*, 3270–3274.
van der Rest, M., & Gingras, G. (1974) *J. Biol. Chem. 249*, 6446–6453.
Won, Y., & Friesner, R. A. (1988) *Isr. J. Chem. 28*, 167–172.
Yeates, T. O., Komiya, H., Chirino, A., Rees, D. C., Allen, J. P., & Feher, G. (1988) *Proc. Natl. Acad. Sci. U.S.A. 85*, 7993–7997.
Yen, H.-C., & Marrs, B. L. (1977) *Arch. Biochem. Biophys. 181*, 411–418.
Youvan, D. C., & Marrs, B. L. (1984) *Cell 39*, 1–4.
Youvan, D. C., Ismail, S., & Bylina, E. J. (1985) *Gene 38*, 19–30.
Zoller, M. J., & Smith, M. (1984) *DNA 3*, 479–488.

Analysis of Photoaffinity-Labeled Aryl Hydrocarbon Receptor Heterogeneity by Two-Dimensional Gel Electrophoresis†

Gary H. Perdew* and Clayton E. Hollenback
Department of Foods and Nutrition, Purdue University, West Lafayette, Indiana 47907
Received July 5, 1989; Revised Manuscript Received January 16, 1990

ABSTRACT: The level of charge heterogeneity in the aryl hydrocarbon receptor (AhR) was examined by high-resolution denaturing two-dimensional (2D) gel electrophoresis. Hepa 1c1c7 cell cytosolic fraction was photoaffinity-labeled with 2-azido-3-[^{125}I]iodo-7,8-dibromodibenzo-*p*-dioxin and applied to isoelectric focusing (IEF) tube gels. After optimization of focusing conditions a broad peak of radioactivity was detected in the apparent p*I* range of 5.2–5.7. IEF tube gels were subjected to sodium dodecyl sulfate–polyacrylamide gel electrophoresis followed by visualization of the radiolabeled AhR by autoradiography; three distinct isoforms were detected. The same 2D electrophoretic isoform pattern was obtained when the AhR from Hepa 1c1c7 was photoaffinity-labeled in cell culture. BP^{r}C1 cells, a mutant line derived from Hepa 1c1c7 cells, contain an AhR that is unable to bind to DNA. Photoaffinity-labeled BP^{r}Cl cytosolic fractions were subjected to 2D gel electrophoretic analysis resulting in essentially the same molecular weight and isoform pattern as seen in Hepa 1c1c7 cytosol. This result would suggest that if a mutation is present in the BP^{r}Cl AhR it has not caused a significant change in its IEF pattern, although a small shift in the p*I* values was observed. Two-dimensional gel electrophoresis of photoaffinity-labeled cytosolic fractions from HeLa cells, the rat liver tumor cell line McA-RH7777, and buffalo rat thymus revealed three isoforms, essentially the same isoform pattern as in Hepa 1c1c7 cells. This would indicate that despite the considerable molecular weight polymorphism between species the level of charge heterogeneity is highly conserved.

The effects of both halogenated and nonhalogenated polycyclic aromatic hydrocarbons are of concern because of their widespread distribution as contaminants in the environment (Young et al., 1983). For example, the use of brominated fire retardants in the manufacturing of carpets, plastics, and textiles is a major source of waste products taken to municipal incinerators. During combustion of these products brominated dioxins and dibenzofurans are produced and can be found in the fly ash, usually disposed of in landfills (Sovocool et al., 1988). The biological response to halogenated polycyclic aromatic hydrocarbons (e.g., TCDD, TCDF)[1] is thought to be mediated by the *Ah* receptor (AhR) (Safe, 1988). This response is both species- and tissue-specific (Poland et al.,

†This work was supported in part by National Institute of Environmental Health Science Grant ES-04869, American Cancer Society Institutional Grant IN-17, and the Showalter Trust Fund 6056. This is technical paper no. 12061, Indiana Agricultural Experiment Station.

[1] Abbreviations: TCDD, 2,3,7,8-tetrachlorodibenzo-*p*-dioxin; TCDF, 2,3,7,8-tetrachlorodibenzofuran; AhR, Aryl hydrocarbon receptor; HSP90, 90-kDa heat-shock protein; M_r, relative mass; MOPS, 3-(*N*-morpholino)propanesulfonic acid; Hepa 1, mouse hepatoma cell line 1c1c7; NP-40, nonidet P-40; IEF, isoelectric focusing; Tris-HCl, tris(hydroxymethyl)aminomethane hydrochloride; PDA, piperazine diacrylamide; CHAPS, (3-[(3-cholamidopropyl)dimethylammonio] 1-propanesulfonate; IEF–SDS–PAGE, isoelectric focusing in the first dimension, followed by sodium dodecyl sulfate–polyacrylamide gel electrophoresis in the second dimension.

0006-2960/90/0429-6210$02.50/0